Light-induced degeneracy of resonance modes in a nonlinear microcavity coupled with waveguides: application to channel drop filter

Evgeny N. Bulgakov and Almas F. Sadreev*

L.V. Kirensky Institute of Physics, 660036 Krasnoyarsk, Russia
**Corresponding author: almas@tnp.krasn.ru*

Received May 9, 2013; revised July 12, 2013; accepted August 7, 2013;
posted August 12, 2013 (Doc. ID 190180); published August 29, 2013

We consider a microcavity with degenerate dipole or hexapole eigenmodes. If the cavity is positioned between waveguides, degeneracy is lifted. However, we show that in a nonlinear microcavity the degeneracy is recovered at certain injected power. In application we consider a two-dimensional photonic crystal of GaAs rods holding two parallel waveguides and one defect made of Kerr media. We show that 100% efficiency channel dropping can be attained without a necessity to tune the resonant frequencies of the microcavity.

OCIS codes: (130.5296) Photonic crystal waveguides; (190.3270) Kerr effect; (190.4360) Nonlinear optics, devices; (230.4320) Nonlinear optical devices.
http://dx.doi.org/10.1364/JOSAB.30.002549

1. INTRODUCTION

Microcavities or resonators formed by point defects and waveguides formed by line defects in photonic crystals (PhCs) have been subjects for much research because of their capability to confine photons within a small volume, and they are expected to be key building blocks for miniature photonic functional devices and photonic integrated circuits. Among various PhC-based devices, ultracompact channel drop filters (CDFs) based on resonant coupling between cavity modes of point defects and waveguide modes of line defects have drawn primary interest because of the substantial demand for them in wavelength division multiplexed optical communication systems. For instance, in-plane CDFs composed of two waveguides and two optical resonators have been proposed by Fan and co-workers [1–3].

Many CDF designs with two resonant microcavities in PhCs were studied theoretically and practically in [4–12], where each cavity was represented by a single monopole eigenmode. If a cavity supports two resonances of different symmetry, then the degeneracy of these resonances provides 100% drop efficiency [1,3]. Such filters potentially offer ideal transfer characteristics with the size of a few micrometers. Alternatively, two microcavities can be replaced by a single microcavity with higher-order eigenmodes excited at the operational frequency [13–17]. Then high-efficiency channel dropping could be achieved in some fine designs of the defect system in order to obtain the degeneracy of the modes [1]. A clear channel drop operation was successfully demonstrated by employing an ultrahigh-quality-factor single microcavity and a suitably designed waveguide bend [18].

The presence of continua of the waveguides lifts the degeneracy of the cavity modes. To enforce the exact degeneracy of the two cavity modes, the CDF designs involve inclusions of different materials and very small feature sizes of a few hundredths of the lattice constant. The CDF based on a triangular lattice of air holes does not involve either inclusion of additional materials or an extra small feature size [4,6]. However, those two cavities should be made precisely for ideal filter characteristics, which is a challenge in fabrication. In the present paper we consider a 2D square lattice PhC holding two waveguides and one microcavity made of Kerr media. The cavity is characterized by different eigenmodes, dipole, quadrupole, hexapole, etc. [19], whose degeneracy is lifted because of the waveguides. We show that the degeneracy of resonances can be restored by tuning of injected power when the cavity is fabricated from Kerr media.

2. BASIC EQUATIONS FOR WAVE TRANSMISSION

Let us assume a four-port system that consists of two linear waveguides and one nonlinear optical cavity with some eigenfrequencies belonging to the propagation band of the waveguide. To begin with, we consider dipole modes that would be degenerate if there were no waveguides. As shown in Fig. 1(a) the first mode is even or odd relative to inversion of the x or y axis (the x axis is aligned along the waveguides), while the second mode shown in Fig. 1(b) has opposite symmetry properties. These two modes represent two-dimensional irreducible representation of the group symmetry C_{4v}. A distance between the waveguides and the cavity can be chosen equal to $a, 2a, 3a, \ldots$ where a is the lattice unit of the two-dimensional square lattice PhC. The coupling strength between the cavity eigenmodes and the waveguides decays exponentially with this distance but has no principal importance for the achievement of 100% channel drop efficiency, as will be shown below. In order to demonstrate the last statement, we consider two choices for the distance as shown in Figs. 1(a) and 1(b) and in Figs. 1(c) and 1(d) in which the

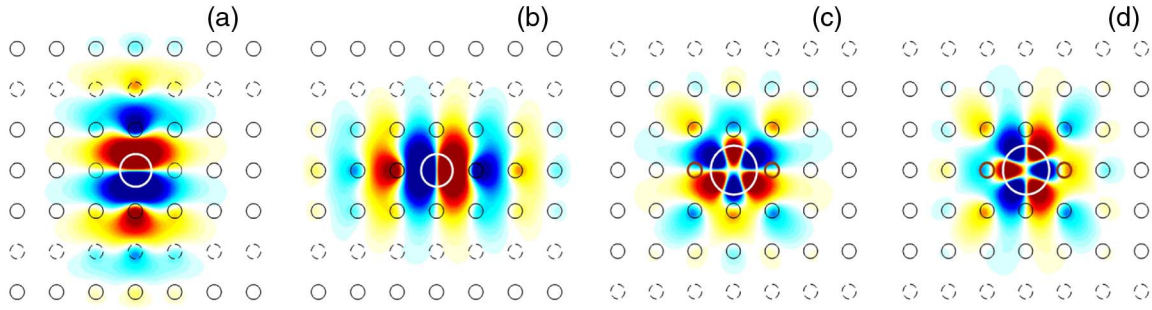

Fig. 1. Microcavity eigenmodes (space profiles of the electric field directed parallel to the rods) in the two-dimensional square lattice PhC consisting of GaAs dielectric rods with radius $0.18a$ and dielectric constant $\epsilon = 11.56$, where $a = 0.5$ μm is the lattice unit [20]. The rods are shown as open gray circles. The defect, shown as the open white circle, has (a), (b) $\epsilon_d = 6.5$ and the radius $r_d = 0.4a$ in the case of dipole modes with eigenfrequency 0.368 and (c), (d) $\epsilon_d = 11.9$ and $r_d = 0.6a$ in the case of hexapole modes with eigenfrequency 0.384. Two rows of rods, shown as dashed open circles, are assumed to be removed to fabricate two parallel waveguides.

coupling strengths differ by 1 order of magnitude. The size and dielectric constant of the defect rod represented by the white circle in Fig. 1 were chosen with the condition that the eigenfrequencies of the defect cavity fit into the propagation band of the waveguides.

Following [21], we present the PhC design in the scheme shown in Fig. 2 and write the coupled mode theory (CMT) equations for time stationary amplitudes,

$$i\omega|A\rangle = (i\hat{\Omega} + \hat{\Gamma})|A\rangle - \hat{K}^T|S_+\rangle, \tag{1}$$

$$|S_-\rangle = \hat{C}|S_+\rangle + \hat{K}|A\rangle, \tag{2}$$

$$\hat{K}^+\hat{K} = 2\hat{\Gamma}, \qquad \hat{C}\hat{K}^* = -\hat{K}. \tag{3}$$

Here the state vector is $|A\rangle^T = (A_1 \quad A_2)$, $|S_+\rangle^T = (S_{1+} \quad 0 \quad 0 \quad 0)$ is the injecting vector, and $|S_-\rangle^T = (S_{1-} \quad S_{2-} \quad \sigma_{1-} \quad \sigma_{2-})$ is the outgoing vector as shown in Fig. 2. In accordance with Eqs. (2) and (3), we have

$$\hat{C} = \begin{pmatrix} 0 & 1 & 0 & 0 \\ 1 & 0 & 0 & 0 \\ 0 & 0 & 0 & 1 \\ 0 & 0 & 1 & 0 \end{pmatrix}, \qquad \hat{\Gamma} = \begin{pmatrix} 2\gamma_1 & 0 \\ 0 & 2\gamma_2 \end{pmatrix}. \tag{4}$$

Then from Eq. (3) we obtain that the coupling matrix $\hat{K}$ takes the following form:

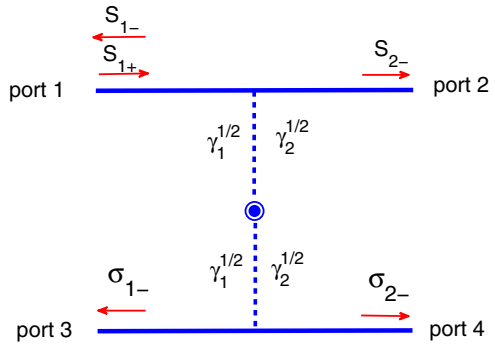

Fig. 2. Four-port system with a nonlinear cavity between two waveguides. $\gamma_1^{1/2}$ and $\gamma_2^{1/2}$ are the coupling constants between waveguides and eigenmodes.

$$\hat{K} = \begin{pmatrix} i\sqrt{\gamma_1} & -\sqrt{\gamma_2} \\ i\sqrt{\gamma_1} & \sqrt{\gamma_2} \\ -i\sqrt{\gamma_1} & -\sqrt{\gamma_2} \\ -i\sqrt{\gamma_1} & \sqrt{\gamma_2} \end{pmatrix}. \tag{5}$$

Finally, substituting Eqs. (4) and (5) into Eq. (1) and taking into account the nonlinearity of the cavity, we have the following equations for the eigenmode amplitudes A_1, A_2 [22]:

$$\begin{aligned} &[\omega - \omega_1 + \lambda_{11}|A_1|^2 + \lambda_{12}|A_2|^2 + 2i\gamma_1]A_1 \\ &\quad + 2\lambda_{12}\,\mathrm{Re}(A_1^*A_2)A_2 = -\sqrt{\gamma_1}S_{1+}, \\ &2\lambda_{12}\,\mathrm{Re}(A_1^*A_2)A_1 + [\omega - \omega_2 + \lambda_{22}|A_2|^2 + \lambda_{12}|A_1|^2 \\ &\quad + 2i\gamma_2]A_2 = -i\sqrt{\gamma_2}S_{1+}, \end{aligned} \tag{6}$$

where $\omega_{1,2}$ are the eigenfrequencies of the cavity modes shifted because of coupling to the waveguides, while

$$\lambda_{mn} = \frac{c^2 n_2^2}{a^2}\int E_m^2(x,y)E_n^2(x,y)\mathrm{d}x\mathrm{d}y, \tag{7}$$

are the nonlinearity constants. The eigenmodes are normalized as follows:

$$\frac{cn_2}{a^2}\int \varepsilon_{\mathrm{PhC}}E_m(x,y)E_n(x,y)\mathrm{d}x\mathrm{d}y = \delta_{mn}, \tag{8}$$

where $\varepsilon_{\mathrm{PhC}}$ is the dielectric constant of the defectless PhC. Integration is performed over the cross section of the nonlinear defect rod with the nonlinear refractive index n_2. The frequencies, the resonance widths, and the nonlinear constants are given in terms of $2\pi c/a$, while $E_m(x,y)$ are the eigenmodes shown in Fig. 1. After substitution of Eqs. (4) and (5) into Eq. (2) we obtain the following equations for the outgoing transmission amplitudes:

$$\begin{aligned} S_{1-} &= i\sqrt{\gamma_1}A_1 - \sqrt{\gamma_2}A_2, \\ S_{2-} &= S_{1+} + i\sqrt{\gamma_1}A_1 + \sqrt{\gamma_2}A_2, \\ \sigma_{1-} &= -i\sqrt{\gamma_1}A_1 - \sqrt{\gamma_2}A_2, \\ \sigma_{2-} &= -i\sqrt{\gamma_1}A_1 + \sqrt{\gamma_2}A_2. \end{aligned} \tag{9}$$

It immediately follows from Eqs. (6) and (9) that the channel dropping is possible only from port 1 into port 3, i.e., $S_{1-} = S_{2-} = \sigma_{2-} = 0$, $\sigma_{1-} = S_{1+}$. That gives us

$$i\sqrt{\gamma_1}A_1 = \sqrt{\gamma_2}A_2 = -\frac{1}{2}S_{1+}; \tag{10}$$

therefore $\mathrm{Re}(A_1^* A_2) = 0$ in Eq. (6). Then, from Eqs. (6) and (10), we obtain that the frequencies become equal to each other when the following condition is fulfilled: $\omega_1 - \lambda_{11}|A_1|^2 - \lambda_{12}|A_2|^2 = \omega_2 - \lambda_{22}|A_2|^2 - \lambda_{12}|A_1|^2$. Obviously, for the circular cross section of a defect rod, $\lambda_{11} = \lambda_{22}$. We assume that this equality holds even for elliptic cross sections with slightly different semiaxes. Note that from Eqs. (7) it follows that $\lambda_{11} > \lambda_{12}$. Then we find values of the injected light power,

$$|S_{1+}|^2 = \frac{4\gamma_1\gamma_2(\omega_2 - \omega_1)}{(\lambda_{11} - \lambda_{12})(\gamma_1 - \gamma_2)} \tag{11}$$

and frequency

$$\omega = \omega_1 - \frac{(\omega_2 - \omega_1)(\lambda_{11}\gamma_2 + \lambda_{12}\gamma_1)}{(\lambda_{11} - \lambda_{12})(\gamma_1 - \gamma_2)}, \tag{12}$$

at which we obtain perfect 100% CDF efficiency from port 1 into port 3.

Equation (11) shows the most important property of the nonlinear cavity coupled with linear waveguides, namely, that the degeneracy of resonances can be restored by the electromagnetic power injected into the waveguide for *arbitrary* eigenfrequencies ω_1, ω_2 and coupling constants γ_1, γ_2. Also one can see that the greater the difference between resonance frequencies $\omega_2 - \omega_1$, the more power must be injected in order to restore a degeneracy. The only condition is $\omega_1 < \omega_2, \gamma_1 > \gamma_2$ or $\omega_1 > \omega_2, \gamma_1 < \gamma_2$. This yields a result important for application in channel dropping, as will be shown below.

3. LIGHT-INDUCED RECOVERY OF DEGENERACY OF RESONANCE DIPOLE OR HEXAPOLE MODES OF A NONLINEAR CAVITY

Let us first consider the dipole modes shown in Figs. 1(a) and 1(b). One can see that the first mode, which is even relative to the x axis, has a larger coupling constant with the waveguide than the second mode. Therefore we have $\gamma_1 > \gamma_2$ and $\omega_1 > \omega_2$, at least for the circular defect rod. Numerical solution of Maxwell's equations shows that the isolated linear defect rod cavity is degenerate with the eigenfrequency $\omega_0 = 0.368$. After removing two rows of the rods, as shown in Figs. 1(a) and 1(b), we obtained $\omega_1 = 0.3692$, $\omega_2 = 0.3653$, $\gamma_1 = 0.0012$, $\gamma_2 = 8 \times 10^{-6}$. Therefore the CDF efficiency will be damaged for the linear circular defect because of the lack of degeneracy of resonant modes. Indeed, Fig. 3 demonstrates that transmission into port 3 achieves only 45% efficiency for the specific PhC design presented in Fig. 1(a). Note that, for these calculations, we take the dielectric constant of the GaAs rods and defect rod as independent of frequency.

For the nonlinear defect the inequalities $\gamma_1 > \gamma_2$, $\omega_1 > \omega_2$ present the "bad" case according to Eq. (11). However, the case can be changed to the "good" one if one takes the defect of an elliptic or rectangular cross section. If we were to take, for example, major and minor semiaxes $0.43a$ and $0.4a$, respectively, for the elliptic cross section of the defect rod, we obtain $\omega_1 = 0.3626$, $\omega_2 = 0.3642$, and $\gamma_1 = 0.0012$, $\gamma_2 = 8 \times 10^{-6}$, which conforms to the inequalities necessary for the CDF. The major semiaxis is aligned across the waveguides. We stress that, although we have changed the cross section of the defect rod, there is no necessity to precisely tune the resonance frequencies by special designs of the PhC structure.

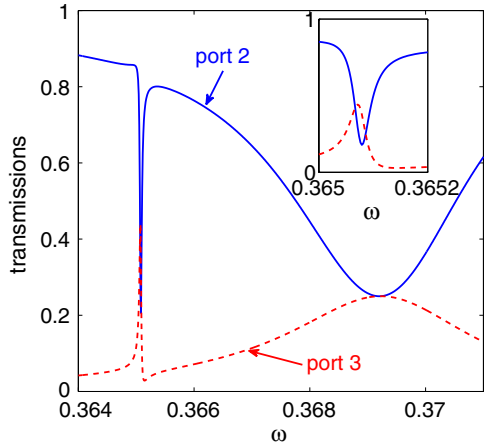

Fig. 3. Transmission spectrum via the dipole modes of a linear microcavity. The defect rod with dielectric constant $\epsilon_d = 6.5$ has a circular cross section with radius $0.4a$.

As a result, for the linear elliptic defect rod we obtain inversion of the resonance frequencies, as seen from Fig. 4(a), compared to the former case of the circular defect rod shown in Fig. 3. In the same PhC design the frequency behavior of the transmission into port 3 for the linear case substantially differs from the case of a nonlinear defect rod, as Figs. 4(a) and 4(b) show. The wide resonance peak does not undergo visible changes, but the narrow resonance peak undergoes a large shift, the value of which depend on at least three factors: the nonlinearity constant λ, the resonance width γ_2, and the injected power P_0 in the universal ratio $P_0\lambda_{22}/\gamma_2$ [20,23]. For the given nonlinearity constant and optimal injected power, Eq. (11), the shift can be estimated as $4(\omega_2 - \omega_1) \sim 10^{-3}$, which agrees with the numerical result shown in Fig. 4(b). This value also evaluates the frequency region of high efficiency of the channel dropping. The 100% CDF efficiency occurs at those frequencies of injected light at which the degeneracy is recovered, as shown in Fig. 4(b). Figure 4(c) shows the transmission into port 4. In both Figs. 4(b) and 4(c) we mark the stable solution of Eq. (6) with open circles.

Next, we compared the CMT results for the transmissions with the numerical solution of the nonlinear Maxwell equations [shown as dashed curves in Figs. 4(b) and 4(c)]. The method for solving the Maxwell equations is described in the appendix of [24]. There is qualitative agreement between the CMT and numerics in the frequency dependence of transmissions into ports 3 and 4. However the CMT and Maxwell equations give different frequency windows and positions where the high CDF efficiency exists. This difference is a result of neglecting radiation shifts in resonance frequencies in the CMT equations, Eqs. (6), which are due to the coupling of the cavity dipole eigenmodes with the waveguides. Moreover in the CMT consideration we have neglected the contribution of other eigenmodes of the resonance nonlinear cavity. Finally, in Fig. 4(d) we show perfect channel dropping as

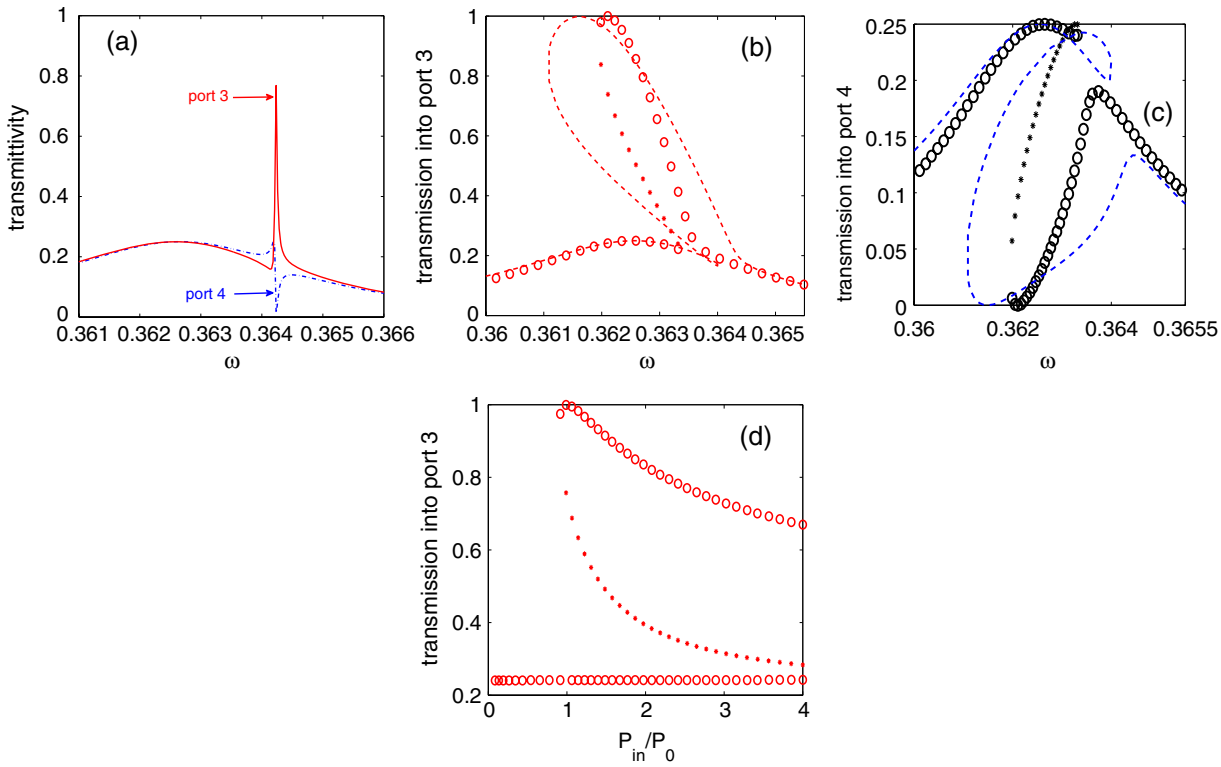

Fig. 4. Transmission spectra into ports 3 and 4 via the dipole modes of the defect cavity. The defect rod with dielectric constant $\epsilon_d = 6.5$ has an elliptic cross section with major and minor semiaxes $0.43a$ and $0.4a$. (a) Linear defect; (b), (c) nonlinear defect with $n_2 = 2 \times 10^{-13}$ cm^2/W for $P_0 = 0.35$ W/a. (d) The transmission from port 1 into port 3 versus the intensity of injected light for $\omega = \omega_c = 0.3621$. Open circles mark the stable solution, and asterisks mark the unstable solution of Eqs. (6). The dashed curves show the solution of the nonlinear Maxwell equations.

an effect of injected light intensity, in full correspondence with Eq. (11).

The first dipole mode [Fig. 1(a)] has coupling constant γ_1, which exceeds the coupling constant γ_2 of the second dipole mode by 2 orders of magnitude. The higher eigenmodes have more nodal lines that decrease this difference. An example of higher hexapole modes is shown in Figs. 1(c) and 1(d). For the same design of PhC the coupling constants are $\gamma_1 = 1.2 \times 10^{-5}$, $\gamma_2 = 2.8 \times 10^{-6}$. For the linear case the design has to be optimized in order to achieve channel dropping [1,13,15]. As in the case of dipole modes, we show that there is no necessity to optimize the design in the nonlinear case. However, neighboring rods, shown in Figs. 1(c) and 1(d) by brown circles, are shifted toward the nonlinear defect in order to achieve $\omega_2 > \omega_1$. However, in contrast to the linear case, the shift can be arbitrary. To be specific, we take the shift $0.03a$ or $-0.03a$ for the left or right neighbor of the defect cavity. That gives only 25% CDF efficiency in the linear case, as shown in Fig. 6(a). The nonlinearity of the defect rod gives 100% efficiency of transmission from port 1 into port 3, as Fig. 6(b)

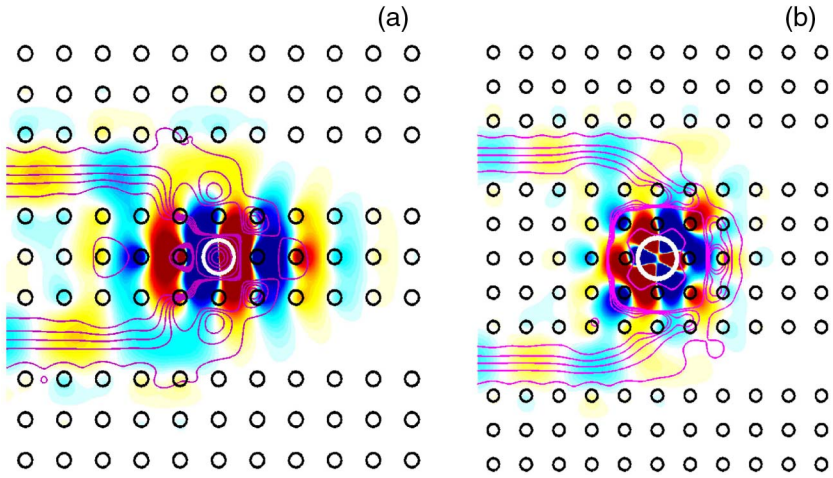

Fig. 5. Real part of the scattering wave function (electric field) in the PhC, which holds two parallel waveguides and one nonlinear cavity with two (a) dipole and (b) hexapole eigenmodes. Injected power and frequency obey the conditions for 100% channel dropping. Pink curves are optical streamlines.

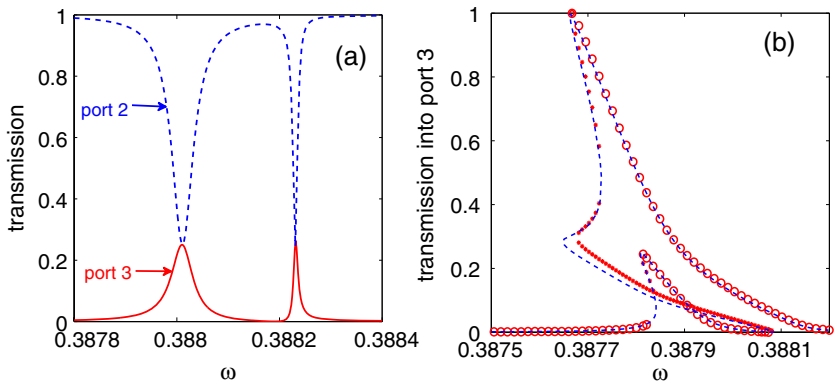

Fig. 6. Transmission spectra via two hexapole modes of a defect cavity. The defect rod with dielectric constant $\epsilon_d = 11.9$ has a circular cross section with radius $0.6a$ but is shifted by $\pm 0.03a$. (a) Linear defect. (b) Nonlinear defect with $n_2 = 2 \times 10^{-13}$ cm^2/W modes for $P_0 = 0.4$ W/a. Dashed curves show the solution of the nonlinear Maxwell equations, and open circles mark the stable solution, while asterisks mark the unstable solution of the CMT equation [Eq. (6)].

demonstrates. Two hexapole modes have the eigenfrequencies $\omega_1 = 0.38791$, $\omega_2 = 0.38813$. Figure 6(a) shows the resonant peaks in the transmission from port 1 into port 3. One can see that only these two eigenhexapole modes participate in the transmission. Next, one can see from Fig. 6(b) that there are two stable solutions around the frequency 0.3621, one with the 100% CDF efficiency, the other with almost 0% efficiency. This result opens a way for all-optical switching of the CDF efficiency from zero to 100% by applying impulses of the injected light, as was demonstrated in [22].

Our numerical calculation of the nonlinear Maxwell equations gives the results close to the results obtained from the CMT equations. These data are shown in Fig. 5(b). The channel dropping is visualized by optical streamlines. The transmission from port 1 into port 3, shown in Fig. 6(b) by the dashed curve, perfectly coincides with the self-consistent solution of the CMT equations, unlike the case of dipole eigenmodes. This is because the coupling of higher-order hexapole eigenmodes of the cavity with the waveguides is weaker than those of the dipole eigenmodes.

4. SUMMARY AND DISCUSSION

In this paper we have demonstrated how nonlinearity can solve the problem of tuning resonant frequencies of a defect microcavity between two linear waveguides by use of a defect rod made from Kerr media. Although originally the cavity modes, dipole, quadrupole, etc., are degenerate, their coupling with continua of waveguides lifts the degeneracy of resonant frequencies. The recovery of the degeneracy requires special optimization of the PhC CDF design, including different materials with precise substitution of positions and sizes for the linear cavity.

In the nonlinear case the degeneracy of resonant modes can be recovered by tuning of injected power or frequency of injected light, as implied by Eqs. (11) and (12) derived in the framework of CMT. These results are in good agreement with direct calculations of the nonlinear Maxwell equations, especially for the hexapole eigenmodes of the nonlinear cavity. Although theoretically we can achieve 100% channel drop efficiency, there are hindrances that can affect that. The first hindrance is related to losses of the EM power for transmission through the waveguides and in the cavity due to vertical emission of light. These losses will damage the channel drop efficiency [3]. The second potential problem is related to a contribution of other eigenmodes of the resonance nonlinear cavity; these modes have an exponentially small contribution in the CMT equations (6). Note that for numerical solution of the Maxwell equations the contribution of other eigenmodes is taken into account that can be a source of discrepancy between the CMT and numerics seen in Figs. 4(b) and 4(c). Equation (11) reveals one important aspect of the light-induced degeneracy of the eigenmodes of the resonant cavity. Assume that the first mode is coupled with ports more than the second. Then the radiation shifts and resonance widths obey the inequalities $\Delta\omega_1 > \Delta\omega_2$ and $\gamma_1 > \gamma_2$. If the eigenmodes were degenerated for the free, say, cylindrical cavity, we obtain that the resonance frequencies obey $\omega_1 > \omega_2$. As a result, Eq. (11) cannot be satisfied. Therefore we had to lift the degeneracy of the free cavity in order to achieve the inequality $\omega_1 < \omega_2$ by, for example, deforming the cylindrical shape of the cavity into an elliptic shape. Specifically, we have taken major and minor semiaxes $0.43a$ and $0.4a$. However, the value of deformation has no importance, which reveals an advantage of the light-induced tuning of the resonance frequencies compared with the linear cavity, where precise tuning of resonant frequencies is necessary. Thus, the light-induced recovery of degeneracy is completely robust relative to errors in fabrication of the PhC design. Moreover, if the nonlinear refractive index is negative, then condition (11) is satisfied even for a cylindrical defect rod (the "good" case).

ACKNOWLEDGMENTS

We thank D. N. Maksimov for critical reading of manuscript and assistance. The work is partially supported by RFBR grant 13-02-00497 and the Integration Project of the Siberian Branch of the RAS (Project No. 29).

REFERENCES

1. S. Fan, P. R. Villeneuve, J. D. Joannopoulos, and H. A. Haus, "Channel drop filters in photonic crystals," Opt. Express **3**, 4–11 (1998).
2. S. Fan, P. R. Villeneuve, J. D. Joannopoulos, M. J. Khan, C. Manolatou, and H. A. Haus, "Theoretical analysis of channel drop tunneling processes," Phys. Rev. B **59**, 15882–15892 (1999).
3. C. Manolatou, M. J. Khan, S. Fan, P. R. Villeneuve, H. A. Haus, and J. D. Joannopoulos, "Coupling of modes analysis of resonant channel add-drop filters," IEEE J. Quantum Electron. **35**, 1322–1331 (1999).

4. M. Qiu and B. Jaskorzynska, "Design of a channel drop filter in a two-dimensional triangular photonic crystal," Appl. Phys. Lett. **83**, 1074–1076 (2003).
5. B. K. Min, J. E. Kim, and H. Y. Park, "Channel drop filters using resonant tunneling processes in two-dimensional triangular lattice photonic crystal slabs," Opt. Commun. **237**, 59–63 (2004).
6. Z. Zhang and M. Qiu, "Small-volume waveguide-section high Q microcavities in 2D photonic crystal slabs," Opt. Express **12**, 3988–3995 (2004).
7. Y. Akahane, T. Asano, H. Takano, B.-S. Song, Y. Takana, and S. Noda, "Two-dimensional photonic-crystal-slab channel-drop filter with flat-top response," Opt. Express **13**, 2512–2530 (2005).
8. K. H. Hwang and G. H. Song, "Design of a high-*Q* channel add-drop multiplexer based on the two-dimensional photonic-crystal membrane structure," Opt. Express **13**, 1948–1957 (2005).
9. A. Shinya, S. Mitsugi, E. Kuramochi, and M. Notomi, "Ultrasmall multi-channel resonant-tunneling filter using mode gap of width-tuned photonic-crystal waveguide," Opt. Express **13**, 4202–4209 (2005).
10. M. Djavid, A. Ghaffari, F. Monifi, and M. S. Abrishamian, "Heterostructure photonic crystal channel drop filters using mirror cavities," J. Opt. A **10**, 055203 (2008).
11. K. Fasihi and S. Mohammadnejad, "Highly efficient channel-drop filter with a coupled cavity-based wavelength-selective reflection feedback," Opt. Express **17**, 8983–8997 (2009).
12. J.-X. Fu, J. Lian, R.-J. Liu, L. Gan, and Z.-Y. Li, "Unidirectional channel-drop filter by one-way gyromagnetic photonic crystal waveguides," Appl. Phys. Lett. **98**, 211104 (2011).
13. J. Romero-Vivas, D. N. Chigrin, A. V. Lavrinenko, and C. M. S. Torres, "Resonant add-drop filter based on a photonic quasicrystal," Opt. Express **13**, 826–835 (2005).
14. Z. Zhang and M. Qiu, "Compact in-plane channel drop filter design using a single cavity with two degenerate modes in 2D photonic crystal slabs," Opt. Express **13**, 2596–2604 (2005).
15. A. D'Orazio, M. De Sario, V. Marrocco, V. Petruzzelli, and F. Prudenzano, "Photonic crystal drop filter exploiting resonant cavity configuration," IEEE Trans. Nanotechnol. **7**, 10–13 (2008).
16. L. Shang, A. Wen, B. Li, and T. Wang, "Coupled spiral-shaped microring resonator-based unidirectional add–drop filters with gapless coupling," J. Opt. **13**, 015503 (2011).
17. Y.-N. Zhao, K.-Z. Li, X.-H. Wang, and C.-J. Jin, "A compact in-plane photonic crystal channel drop filter," Chin. Phys. B **20**, 047210 (2011).
18. H. Takano, B.-S. Song, T. Aasano, and S. Noda, "Highly effective in-plane channel-drop filters in two-dimensional heterostructure photonic-crystal slab," Jpn. J. Appl. Phys. **45**, 6078–6086 (2006).
19. J. Joannopoulos, R. D. Meade, and J. Winn, *Photonic Crystals* (Princeton University, 1995).
20. M. Soljačić, M. Ibanescu, S. G. Johnson, Y. Fink, and J. D. Joannopoulos, "Optimal bistable switching in nonlinear photonic crystals," Phys. Rev. E **66**, 055601(R) (2002).
21. W. Suh, Z. Wang, and S. Fan, "Temporal coupled-mode theory and the presence of non-orthogonal modes in lossless multimode cavities," IEEE J. Quantum Electron. **40**, 1511–1518 (2004).
22. E. N. Bulgakov and A. F. Sadreev, "Symmetry breaking in photonic crystal waveguide coupled with the dipole modes of a nonlinear optical cavity," J. Opt. Soc. Am. B **29**, 2924–2928 (2012).
23. M. F. Yanik, S. Fan, and M. Soljačić, "High-contrast all-optical bistable switching in photonic crystal microcavities," Appl. Phys. Lett. **83**, 2739–2741 (2003).
24. E. N. Bulgakov and A. F. Sadreev, "All-optical manipulation of light in X- and T-shaped photonic crystal waveguides with a nonlinear dipole defect," Phys. Rev. B **86**, 075125 (2012).